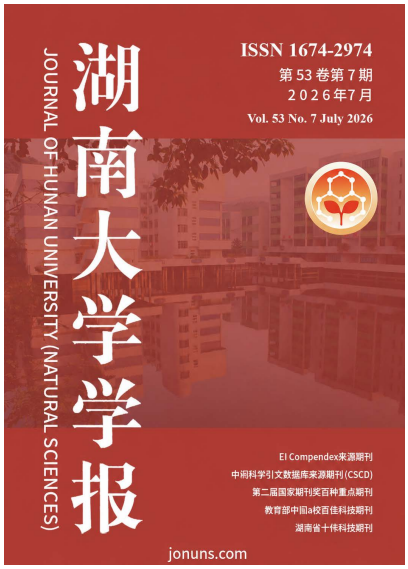

Journal of Hunan University (Natural Sciences)

Vol. 53 No. 7

July 2026

Available online at

https://jonuns.com

Open Access Article

https://doi.org/10.55463/issn.1674-2974.53.7.2

Enzymatic Deglycosylation of Hederacoside C Yields Potent Anti-inflammatory Metabolites for Inflammatory Bowel Disease

Qiongming Xu [1]*, Sabiqun Nahar Bithy [1], Ra Ade Hossain [2], Jianqin Zhou [1], Yanli Liu [1]

[1] School of Pharmaceutical Sciences, Soochow University, Suzhou 215123, China,

[2] School of Metallurgy and Environment, Changsha Central South University, Changsha 430001, China,

* Corresponding author: xuqiongming@suda.edu.cn, sabiqunbithu97@gmail.com

Article History:

Received: May 26, 2026
Revised: June 27, 2026
Accepted: July 6, 2026
Published: July 20, 2026

Abstract: Hederacoside C (HDC), a pentasaccharide triterpenoid saponin isolated from *Pulsatilla chinensis* (Bunge) Regel, has documented anti-inflammatory activity but limited oral bioavailability because of its high hydrophilicity. This study investigated whether enzymatic deglycosylation could generate HDC metabolites with enhanced anti-inflammatory activity. Using α-L-rhamnosidase (RhaK), three principal deglycosylated metabolites, designated HDC-1–HDC-3, were generated and characterized. In lipopolysaccharide-stimulated RAW 264.7 macrophages, HDC-1 and HDC-3 exhibited greater anti-inflammatory activity than the parent compound, as demonstrated by stronger suppression of the pro-inflammatory cytokines IL-1β and IL-6. Although HDC-3 showed the highest in vitro activity, HDC-1 was selected for in vivo evaluation because it combined substantial biological activity with a higher preparative yield and greater scalability. In a dextran sulfate sodium-induced murine colitis model, intraperitoneal administration of HDC-1 at 1.25, 2.5, and 5 mg/kg dose-dependently reduced body-weight loss and disease activity, preserved colon length, decreased colonic IL-1β and IL-6 levels, and improved

histopathological injury. Under the tested dosing regimens, HDC-1 produced greater therapeutic effects than oral HDC at 100 mg/kg and mesalazine at 200 mg/kg. These findings identify HDC-1 as a promising deglycosylated lead compound and support enzymatic biotransformation as a scalable strategy for developing potent saponin-derived candidates for the treatment of inflammatory bowel disease.

Keywords: Hederacoside C; enzymatic deglycosylation; α-L-rhamnosidase; triterpenoid saponin; DSS-induced colitis; anti-inflammatory activity; inflammatory bowel disease.

常春藤皂苷C酶法脱糖生成具有强效抗炎活性的炎症性肠病候选代谢产物

摘要： 常春藤皂苷C（Hederacoside C，HDC）是一种从白头翁（Pulsatilla chinensis (Bunge) Regel）中分离得到的五糖型三萜皂苷，具有明确的抗炎活性，但由于其亲水性较强，口服生物利用度较低。本研究旨在考察酶法脱糖是否能够生成具有更强抗炎活性的HDC代谢产物。采用α-L-鼠李糖苷酶（RhaK）制备并表征了三种主要脱糖代谢产物，分别命名为HDC-1、HDC-2和HDC-3。在脂多糖刺激的RAW 264.7巨噬细胞中，HDC-1和HDC-3表现出较母体化合物HDC更强的抗炎活性，具体表现为对促炎性细胞因子IL-1β和IL-6更显著的抑制作用。尽管HDC-3在体外实验中表现出最高活性，但由于HDC-1兼具较强的生物活性、较高的制备得率和更好的规模化生产潜力，因此被选用于体内评价。在葡聚糖硫酸钠诱导的小鼠结肠炎模型中，腹腔注射HDC-1（1.25、2.5和5mg/kg）可剂量依赖性地减轻体重下降和疾病活动程度，维持结肠长度，降低结肠组织中IL-1β和IL-6水平，并改善组织病理学损伤。在本研究所采用的给药方案下，HDC-1的治疗效果优于口服HDC（100mg/kg）和美沙拉嗪（200 mg/kg）。上述结果表明，HDC-1是一种具有开发潜力的脱糖先导化合物，同时支持将酶促生物转化作为一种可规模化策略，用于开发治疗炎症性肠病的高活性皂苷衍生候选药物。

关键词： 常春藤皂苷C；酶法脱糖；α-L-鼠李糖苷酶；三萜皂苷；DSS诱导性结肠炎；抗炎活性；炎症性肠病。

1. Introduction

Inflammatory bowel disease (IBD) comprises two major chronic and relapsing inflammatory disorders of the gastrointestinal tract: ulcerative colitis (UC) and Crohn's disease (CD) [1–6]. UC is characterized by continuous mucosal inflammation that typically begins in the rectum and extends proximally through the colon, whereas CD may affect any part of the gastrointestinal tract and is characterized by discontinuous, transmural inflammation [7–9]. Common clinical manifestations include persistent diarrhea, which is frequently bloody in UC, abdominal pain, rectal bleeding, fecal urgency, fatigue, weight loss, and fever during disease exacerbations. Extraintestinal manifestations may involve the eyes, skin, joints, and hepatobiliary system, while long-standing colonic inflammation is associated with an increased risk of colorectal cancer [10–15]. Collectively, the chronic and unpredictable course of IBD imposes a substantial clinical burden and markedly reduces patients' quality of life.

The pathogenesis of IBD is multifactorial and involves complex interactions among genetic susceptibility, environmental factors, intestinal microbiota dysbiosis, epithelial barrier dysfunction, and dysregulated immune responses. These interacting mechanisms promote sustained activation of inflammatory signaling pathways, including nuclear factor kappa B (NF-κB) and mitogen-activated protein kinase (MAPK), as well as excessive production of pro-inflammatory cytokines such as tumor necrosis factor-α (TNF-α), interleukin-6 (IL-6), and interleukin-1β (IL-1β) [16–20]. Current therapeutic strategies include 5-aminosalicylates, corticosteroids, immunomodulators, biological agents

such as anti-TNF and anti-integrin antibodies, and targeted small-molecule therapies, including Janus kinase inhibitors. However, their clinical effectiveness may be limited by primary non-response, secondary loss of response, treatment-related adverse effects, infections, and, in selected cases, an increased risk of malignancy [21–26]. These limitations highlight the continuing need for therapeutic candidates with improved efficacy, safety, and pharmacological properties.

Natural products remain an important source of structurally diverse bioactive compounds and continue to contribute substantially to modern drug discovery [27–30]. Among them, triterpenoid saponins have attracted considerable attention because of their reported anti-inflammatory, antioxidant, antimicrobial, and immunomodulatory activities [31–33]. Nevertheless, the therapeutic development of many saponins is restricted by their high molecular weight, extensive glycosylation, limited membrane permeability, and poor oral bioavailability.

Hederacoside C (HDC) is a pentasaccharide triterpenoid saponin with a molecular weight of 1221.38 Da that has been isolated from *Pulsatilla chinensis* (Bunge) Regel. HDC has been reported to exhibit anti-inflammatory, antioxidant, antimicrobial, and antispasmodic activities [35–37]. Its anti-inflammatory effects have been associated with the modulation of TLR2- and TLR4-mediated signaling and the inhibition of downstream MAPK and NF-κB pathways [38,39]. In lipopolysaccharide-stimulated macrophages, HDC suppresses the expression of pro-inflammatory mediators, including TNF-α, IL-1β, inducible nitric oxide synthase, and cyclooxygenase-2, while promoting the expression of the anti-inflammatory cytokine IL-10. HDC has also been reported to inhibit S100A9/MAPK signaling, preserve epithelial tight-junction proteins, and attenuate neutrophil recruitment in experimental inflammatory models [40].

Despite these pharmacological activities, HDC exhibits extremely low oral bioavailability, reportedly ranging from 0.118% to 0.250%. This limitation is largely attributable to its high molecular weight and strong hydrophilicity resulting from the presence of five sugar residues [41,42]. Following oral administration, HDC may undergo deglycosylation by intestinal microbial and mammalian glycosidases, generating less glycosylated and potentially more lipophilic metabolites. Such metabolites may exhibit improved membrane permeability, target accessibility, and biological activity compared with the parent compound.

Enzymatic deglycosylation using glycosidases provides a mild, selective, and environmentally sustainable alternative to conventional acid hydrolysis. In particular, α-L-rhamnosidase can selectively cleave terminal rhamnose residues and facilitate the controlled production of structurally defined metabolites while minimizing nonspecific degradation and acidic waste generation [43–47]. Enzymatic transformation has previously been applied to improve the pharmacological properties of several natural glycosides. However, the site-selective preparation of HDC metabolites and the systematic evaluation of their anti-inflammatory activities remain insufficiently investigated.

In the present study, α-L-rhamnosidase RhaK was employed to selectively remove terminal α-L-rhamnose residues from the glycosidic chains attached at the C-3 and C-28 positions of HDC. Three principal deglycosylated metabolites, designated HDC-1, HDC-2, and HDC-3, were generated, isolated, structurally characterized, and evaluated for cytotoxicity and anti-inflammatory activity in vitro. The enzymatic reaction conditions were subsequently optimized to improve the selective production and preparative scalability of the most promising metabolite. HDC-1 was selected for further evaluation on the basis of its combined biological activity, preparative yield, and scalability, and its therapeutic effects were examined in a dextran sulfate sodium-induced murine colitis model. This study therefore aimed to determine whether site-selective enzymatic deglycosylation could enhance the pharmacological properties of HDC and provide a scalable strategy for generating potent saponin-derived candidates for further preclinical development in inflammatory bowel disease. The overall experimental workflow is illustrated in Figure 1.

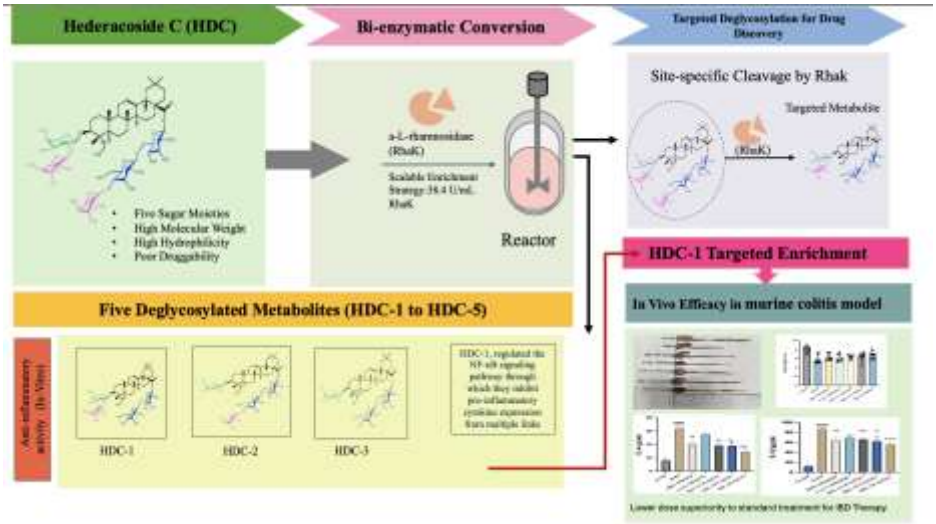

Figure 1. Bi-enzymatic Conversion of Hederacoside C (HDC) into Deglycosylated Metabolites for IBD Therapy

2. Materials and methods

2.1. Materials

Hederacoside C (HDC; purity >98%) was isolated from the dried roots of *Pulsatilla chinensis* (Bunge) Regel using macroporous adsorption resin chromatography followed by preparative high-performance liquid chromatography (HPLC). The identity and purity of HDC were confirmed by HPLC–mass spectrometry (HPLC–MS) and nuclear magnetic resonance (NMR) spectroscopy.

α-L-Rhamnosidase RhaK was obtained from Sunson Industry Group Co., Ltd. (Cangzhou, China). Lipopolysaccharide (LPS; *Escherichia coli* O111:B4) was purchased from Sigma-Aldrich (St. Louis, MO, USA). Mouse interleukin-1β (IL-1β) and interleukin-6 (IL-6) enzyme-linked immunosorbent assay (ELISA) kits were purchased from Thermo Fisher Scientific (Waltham, MA, USA). Unless otherwise specified, all other chemicals and solvents were of analytical grade and were purchased from Sinopharm Chemical Reagent Co., Ltd. (Shanghai, China).

2.2. Animals

Male C57BL/6 mice aged 6–8 weeks and weighing 22 ± 2 g were obtained from the Experimental Animal Center of Soochow University (Suzhou, China). The animals were housed under specific pathogen-free conditions at 22–24°C and 50–60% relative humidity under a 12-h light/dark cycle, with free access to food and water.

All animal procedures were conducted in accordance with the guidelines of the Laboratory Animal Care and Use Committee of the College of Pharmaceutical Sciences, Soochow University, and were approved by the institutional ethics committee.

2.3. Acid Hydrolysis of HDC

Acid hydrolysis was performed by mixing 1 mL of HDC solution (20 mg/mL) with 1 mL of sulfuric acid solution at concentrations of 0.5, 1.0, or 2.0 mol/L in sealed reaction tubes. The reaction mixtures were incubated at 60°C for 8 h. After hydrolysis, 2 mL of methanol was added to each sample. The resulting solutions were filtered through a 0.22-μm membrane and analyzed by HPLC.

Acid hydrolysis produced complex product mixtures with limited selectivity and was therefore considered unsuitable for the preparative production of structurally defined HDC metabolites.

2.4. Enzymatic Deglycosylation of HDC

An HDC solution prepared in ultrapure water at a concentration of 20 mg/mL was mixed with an equal volume of α-L-rhamnosidase RhaK solution (76.8 U/mL) prepared in citrate–phosphate buffer at pH 4.0. The final enzyme concentration in the 2-mL reaction mixture was 38.4 U/mL.

The reaction mixture was incubated at 50°C for 8 h to facilitate the selective removal of terminal rhamnose residues. The enzyme was subsequently inactivated by heating the mixture at 100°C for 30 min. After cooling, an equal volume of methanol was added. The mixture was centrifuged at 5,000 rpm for 15 min, and the resulting supernatant was concentrated under reduced pressure. The samples were then filtered through a 0.22-μm membrane before HPLC analysis.

2.5. HPLC Analysis

HDC and its deglycosylated metabolites were analyzed using a Waters e2695 HPLC system equipped with a COSMOSIL 3C_{18}-EB column (150 × 4.6 mm, 10 μm; Nacalai Tesque, Kyoto, Japan).

The mobile phase consisted of deionized water as solvent A and acetonitrile as solvent B. The flow rate was maintained at 0.6 mL/min. The gradient elution program was as follows: 0–20 min, 28–33%

B; 20–30 min, 33–34% B; and 30–31 min, 34–28% B, followed by re-equilibration at 28% B. The column temperature was maintained at 25°C, the injection volume was 10 μL, and chromatographic detection was performed at 203 nm.

2.6. Preparative Isolation of Deglycosylated Metabolites

Deglycosylated HDC metabolites were isolated using a Huitong preparative HPLC system (Soochow High-Tech Chromatography Co., Ltd., Suzhou, China) equipped with a ChromCore 120 HP C_{18} column (250 × 30 mm, 10 μm; NanoChrom Technologies, China).

The mobile phase consisted of deionized water as solvent A and acetonitrile as solvent B, with a flow rate of 8 mL/min. The preparative gradient was as follows: 0–40 min, 28–33% B; 40–48 min, 33–34% B; and 48–60 min, return to the initial mobile-phase composition for column re-equilibration. The injection volume was 5 mL, and detection was performed at 203 nm.

Fractions corresponding to the principal deglycosylated metabolites were collected, concentrated by rotary evaporation, and freeze-dried. The isolated products were subsequently subjected to structural characterization and biological activity assays.

2.7. Structural Identification of Deglycosylated Metabolites

The structures of the isolated metabolites were determined using NMR spectroscopy and high-resolution mass spectrometry (HR-MS). ^1H NMR and ^13C NMR spectra were recorded using a Bruker AVANCE III 400 MHz spectrometer (Bremen, Germany), with pyridine-d_5 or methanol-d_4 used as the solvent.

High-resolution mass spectra were acquired using an LTQ Orbitrap Elite mass spectrometer (Thermo Fisher Scientific, Waltham, MA, USA). Structural assignments were made by comparing the obtained spectroscopic data with previously published data.

The three principal metabolites were identified as follows: HDC-1, resulting from the removal of the terminal rhamnose residue from the C-28 glycosidic chain; HDC-2, resulting from the removal of the terminal rhamnose residue from the C-3 glycosidic chain; and HDC-3, resulting from the removal of terminal rhamnose residues from both glycosidic chains.

2.8. Cell Culture

RAW 264.7 murine macrophages were obtained from the American Type Culture Collection (ATCC, Manassas, VA, USA). Cells were maintained in RPMI 1640 medium supplemented with 10% fetal bovine serum and penicillin–streptomycin. The cells were cultured at 37°C in a humidified atmosphere containing 5% CO_2.

Human intestinal epithelial cells (HIEC) were maintained in Dulbecco's modified Eagle medium supplemented with 10% fetal bovine serum and 1% penicillin–streptomycin under the same incubation conditions.

2.9. Cytotoxicity Assay

RAW 264.7 cells were seeded into 96-well plates at a density of 5 × 10^4 cells per well and allowed to adhere for 12 h. The culture medium was subsequently replaced with fresh medium containing HDC or its deglycosylated metabolites at concentrations ranging from 5 to 100 μM. The final concentration of dimethyl sulfoxide (DMSO) did not exceed 0.1%. Control cells received medium containing 0.1% DMSO alone.

After 24 h of exposure, 10 μL of MTT solution (5 mg/mL in phosphate-buffered saline) was added to each well. Following incubation with MTT, the medium was removed, and 100 μL of DMSO was added to dissolve the resulting formazan crystals. Absorbance was measured at 570 nm using a microplate reader. Cell viability was expressed as a percentage of the vehicle-control value.

2.10. Cell Viability Following Erastin-Induced Ferroptosis

HIEC cells were seeded into 96-well plates at a density of 5 × 10^4 cells per well in 100 μL of complete medium and incubated for 16–18 h to allow cell attachment. The culture medium was then replaced with fresh medium containing various concentrations of HDC or its deglycosylated metabolites, up to a maximum concentration of 40 μM.

After pretreatment for 1 h, erastin was added at a final concentration of 6 μM to induce ferroptosis. The cells were incubated for an additional 8 h without replacement of the culture medium. Vehicle-control cells received 0.1% DMSO, while the positive-control group was treated with erastin alone. Additional rescue-control groups were treated with a proteasome inhibitor at 100 μM, ferrostatin-1 at 1 μM, or deferoxamine mesylate at 100 μM.

Cell viability was determined using the Cell Counting Kit-8 assay. Briefly, 10 μL of CCK-8 reagent was added to each well, followed by incubation for 2–3 h. Absorbance was measured at 450 nm using a Bio-Rad microplate reader.

2.11. Measurement of Pro-Inflammatory Cytokines in RAW 264.7 Cells

RAW 264.7 cells were seeded into six-well plates at a density of 1 × 10^6 cells per well and incubated for 12 h at 37°C in a humidified atmosphere containing 5% CO_2.

The experimental groups included a normal-control group, an LPS model group, and treatment groups. Cells in the treatment groups were pretreated

for 1 h with HDC or one of its deglycosylated metabolites, HDC-1, HDC-2, or HDC-3, at a concentration of 10 μM. LPS was subsequently added to the model and treatment groups at a final concentration of 1 μg/mL. The normal-control group received no LPS. The cells were then incubated for an additional 24 h.

Culture supernatants were collected and centrifuged at 3,000 rpm for 5 min to remove cellular debris. IL-1β and IL-6 concentrations were measured using commercial ELISA kits in accordance with the manufacturers' instructions. Absorbance was measured at 450 nm, and cytokine concentrations were calculated using the corresponding standard curves. All experiments were performed in triplicate, and the results are expressed as the mean ± standard deviation.

2.12. Induction of Colitis and Drug Administration

Following a one-week acclimatization period, mice were randomly allocated to the following groups, with eight animals per group:

1. normal-control group;
2. DSS model group;
3. HDC group, treated with 100 mg/kg HDC orally once daily;
4. mesalazine group, treated with 200 mg/kg mesalazine orally once daily;
5. low-dose HDC-1 group, treated with 1.25 mg/kg HDC-1 intraperitoneally twice daily;
6. medium-dose HDC-1 group, treated with 2.5 mg/kg HDC-1 intraperitoneally twice daily;
7. high-dose HDC-1 group, treated with 5 mg/kg HDC-1 intraperitoneally twice daily.

Experimental colitis was induced by administering 3% dextran sulfate sodium in the drinking water for 7 consecutive days to all groups except the normal-control group. Drug administration began on day 0 and continued for 10 consecutive days. The mice were euthanized at the end of the treatment period.

Body weight was recorded daily at 09:00. The percentage change in body weight relative to baseline was calculated as follows:

Body weight change (%) = [(daily body weight − initial body weight) / initial body weight] × 100.

2.13. Disease Activity Index Scoring

The severity of experimental colitis was evaluated daily using the Disease Activity Index (DAI), which incorporated body-weight loss, stool consistency, and rectal bleeding.

Body weight was measured each day at 09:00. Weight loss was scored as follows: no weight loss, 0 points; 1–5% loss, 1 point; 5–10% loss, 2 points; 10–15% loss, 3 points; and >15% loss, 4 points.

Stool consistency was assessed daily and scored as follows: well-formed, hard stool, 0 points; soft but formed stool, 1 point; and unformed or watery stool, 2 points.

Rectal bleeding was initially assessed by visual examination. Grossly visible blood was assigned a score of 2. When no visible blood was detected, a fecal smear was prepared and treated with 2% *o*-toluidine in glacial acetic acid and 3% H_2O_2. The appearance of a blue-green color within 1 min was considered indicative of occult blood and was assigned a score of 1. Samples without visible or occult blood were assigned a score of 0.

The DAI was calculated as the sum of the body-weight-loss, stool-consistency, and rectal-bleeding scores.

2.14. Colon Length and Histopathological Examination

At the end of the 10-day intervention period, the mice were euthanized, and the entire colon was excised. Colon length was measured immediately. Colonic tissues were washed with physiological saline, fixed, dehydrated, embedded in paraffin, and sectioned at a thickness of 4 μm.

The sections were stained with hematoxylin and eosin and examined using a light microscope (DP73, Olympus, Tokyo, Japan) at 200× magnification. Histopathological evaluation focused on mucosal integrity, crypt architecture, inflammatory-cell infiltration, and the presence of ulceration or other tissue damage.

2.15. Measurement of IL-1β and IL-6 in Colonic Tissue

Approximately 50 mg of colonic tissue was minced and homogenized in 1 mL of radioimmunoprecipitation assay lysis buffer supplemented with protease and phosphatase inhibitors. The samples were subsequently subjected to ultrasonication.

The tissue lysates were centrifuged at 12,000 × *g* for 10 min at 4°C to remove insoluble debris. The resulting supernatants were collected, and IL-1β and IL-6 concentrations were determined using commercial ELISA kits according to the manufacturers' protocols.

2.16. Statistical Analysis

All in vitro experiments were performed in at least three independent replicates. Data are presented as the mean ± standard deviation. Statistical analyses were performed using GraphPad Prism version 8.0 (GraphPad Software, La Jolla, CA, USA).

Depending on the experimental design, differences among groups were evaluated using one-way or two-way analysis of variance, followed by an appropriate multiple-comparisons test. The exact post hoc test used must be specified in the final manuscript.

Comparisons between the normal-control and model groups are denoted by number signs, whereas

comparisons between the treatment and model groups are denoted by asterisks. Statistical significance was defined as follows: ^# or $p < 0.05$; ^## or $p < 0.01$; and ^### or $p < 0.001$. Differences with $p \geq 0.05$ were considered statistically nonsignificant.

3. Results and Discussion

3.1. Deglycosylated Metabolites of HDC

3.1.1. Acid Hydrolysis of HDC

Both chemical and enzymatic methods can be used to obtain deglycosylated derivatives of Hederacoside C (HDC). Acid hydrolysis was initially evaluated as a conventional chemical approach. HDC was treated with sulfuric acid at concentrations of 0.5, 1.0, and 2.0 mol/L at 60°C for 8 h.

As shown in Figure 2, sulfuric acid hydrolysis produced five major chromatographic peaks and more than three additional minor peaks, indicating extensive and nonselective degradation of HDC. Increasing the acid concentration did not yield a clearly defined product profile suitable for preparative isolation. In addition, acid hydrolysis generates strongly acidic waste and may require extensive neutralization and downstream purification, thereby creating environmental and operational limitations for large-scale applications. Therefore, acid hydrolysis was not pursued further as a preparative method for producing structurally defined deglycosylated HDC metabolites.

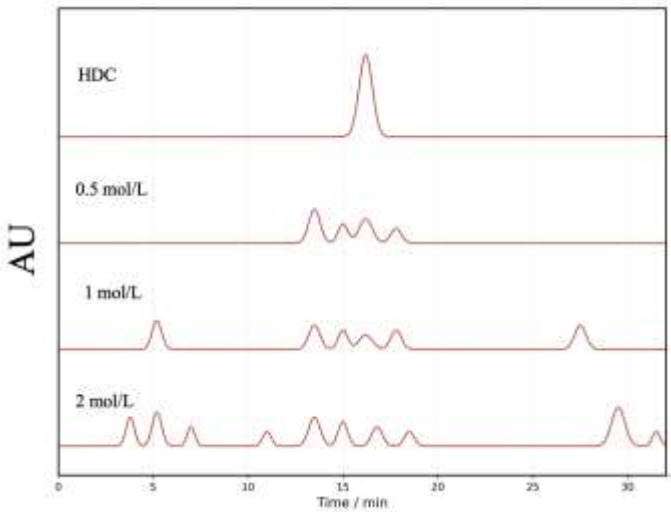

Figure 2. HPLC Chromatograms of HDC hydrolyzed with 0.5, 1 and 2 mol/L sulfuric acids in 8 h

3.1.2. Enzymatic Preparation of Deglycosylated HDC Metabolites

Enzymatic deglycosylation was subsequently evaluated as a more selective and environmentally sustainable approach. The distribution of the resulting metabolites was analyzed by HPLC, as shown in Figure 3a. Hydrolysis of HDC with α-L-rhamnosidase RhaK generated three principal deglycosylated metabolites, designated HDC-1, HDC-2, and HDC-3.

HDC contains terminal rhamnose residues within the glycosidic chains attached at the C-3 and C-28 positions. The three principal metabolites were isolated by preparative HPLC and structurally characterized using high-resolution mass spectrometry and nuclear magnetic resonance spectroscopy. Based on the spectroscopic data, HDC-1 was identified as the product formed by removal of the terminal rhamnose residue from the C-28 glycosidic chain, whereas HDC-2 resulted from removal of the corresponding rhamnose residue from the C-3 glycosidic chain. HDC-3 was generated through the removal of terminal rhamnose residues from both glycosidic chains.

α-L-Rhamnosidases function as exoglycosidases that hydrolyze terminal α-L-rhamnosidic bonds. In the present system, RhaK exhibited differential activity toward the rhamnose residues associated with the C-3 and C-28 glycosidic chains, thereby determining both the composition and relative abundance of the resulting metabolites.

Compared with acid hydrolysis, the enzymatic process proceeded under milder temperature and mildly acidic conditions, minimized nonspecific degradation, and generated a cleaner metabolite profile. These advantages facilitated downstream purification and were consistent with the principles of green chemistry.

The yield of HDC-1 was substantially greater than the combined yields of HDC-2 and HDC-3, as indicated by the HPLC profile in Figure 3a. This finding suggests that RhaK preferentially hydrolyzes the terminal rhamnose residue associated with the C-28 glycosidic chain rather than that associated with the C-3 glycosidic chain. Collectively, these results indicate that the positional selectivity of RhaK is a major determinant of both conversion efficiency and product distribution during the enzymatic biotransformation of HDC.

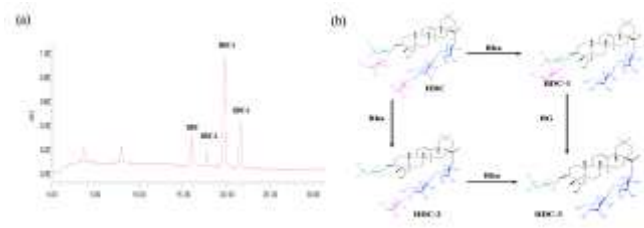

Figure 3. Enzymatic deglycosylation of Hederacoside C by α-L-rhamnosidase RhaK: (a) HPLC chromatograms of HDC and its deglycosylated metabolites after enzymatic hydrolysis; and (b) chemical structures of HDC-1, HDC-2, and HDC-3 and the proposed deglycosylation pathway.

3.1.3. In Vitro Evaluation of the Biological Activities of Deglycosylated HDC Metabolites

The in vitro biological activities of the deglycosylated metabolites of Hederacoside C (HDC) were evaluated using RAW 264.7 murine macrophages, a widely used cellular model for investigating inflammatory responses.

To exclude the possibility that the observed anti-inflammatory effects were attributable to cytotoxicity, HDC and the three principal deglycosylated metabolites, HDC-1, HDC-2, and HDC-3, were initially evaluated using the MTT assay. RAW 264.7 cells were exposed to the test compounds at concentrations of 5, 10, 20, and 100 μM for 24 h. As shown in Figure 4a, none of the tested compounds caused a significant reduction in cell viability compared with the vehicle-control group under the experimental conditions. These results indicate that HDC and its deglycosylated metabolites were not detectably cytotoxic to RAW 264.7 cells within the tested concentration range.

Ferroptosis is an iron-dependent form of regulated cell death characterized by excessive lipid peroxidation and has been implicated in tissue injury and inflammatory disorders [48,49]. To further evaluate the cytoprotective potential of the compounds, an erastin-induced ferroptosis model was established in human intestinal epithelial cells (HIEC), and cell viability was measured using the CCK-8 assay [50–52]. Erastin treatment reduced cell viability to approximately 58% of that observed in the vehicle-control group, confirming successful induction of ferroptotic injury (Figure 4b). Pretreatment with HDC-1 or HDC-3 at 10 μM significantly increased cell viability compared with the erastin-treated model group. These findings suggest that HDC-1 and HDC-3 exert protective effects against erastin-induced ferroptotic injury in intestinal epithelial cells.

Based on the cytotoxicity and cell-protection results, a concentration of 10 μM was selected for subsequent anti-inflammatory evaluation. RAW 264.7 cells were stimulated with lipopolysaccharide (LPS), and the concentrations of the pro-inflammatory cytokines IL-1β and IL-6 in the culture supernatants were determined (Figure 4c,d). LPS stimulation significantly increased IL-1β and IL-6 production compared with the normal-control group, confirming activation of the inflammatory response.

Treatment with the deglycosylated metabolites reduced LPS-induced cytokine production to varying degrees. HDC-1 showed pronounced inhibition of IL-1β production, whereas HDC-3 produced the strongest reduction in IL-6 levels and also significantly suppressed IL-1β. Compared with the parent compound HDC, HDC-3 exhibited a broader anti-inflammatory profile by significantly reducing both cytokines. Collectively, these findings identify HDC-1 and HDC-3 as the most active deglycosylated metabolites in the in vitro assays and support the hypothesis that selective removal of terminal rhamnose residues can enhance the biological activity of HDC.

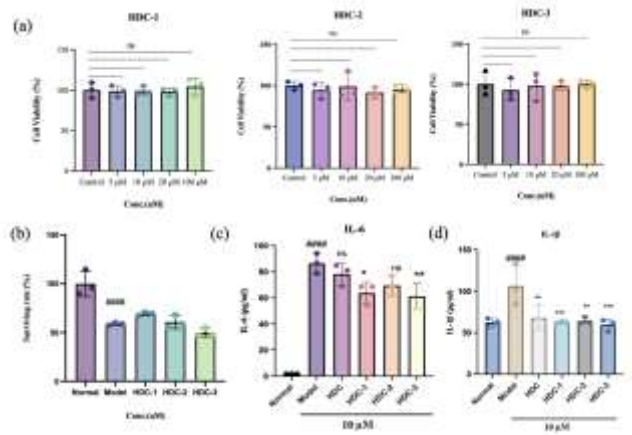

Figure 4. In vitro safety and biological activity of HDC and its deglycosylated metabolites: (a) viability of RAW 264.7 cells following treatment with HDC and its deglycosylated metabolites; (b) protective effects of the test compounds against erastin-induced ferroptotic injury in HIEC cells; (c) effects of the test compounds on LPS-induced IL-6 production in RAW 264.7 cells; and (d) effects of the test compounds on LPS-induced IL-1β production in RAW 264.7 cells. Data are presented as the mean ± standard deviation (n = 3).

Overall, among the three principal deglycosylated metabolites, HDC-1 and HDC-3 exhibited the most consistent biological activity in vitro. HDC-1 showed pronounced protective activity against erastin-induced ferroptotic injury and strongly inhibited IL-1β production, whereas HDC-3 significantly reduced both IL-1β and IL-6 levels and therefore exhibited a broader anti-inflammatory profile. In several assays, these metabolites were more active than the parent compound HDC. These findings indicate that the selective removal of terminal rhamnose residues can enhance the pharmacological activity of HDC and support the further evaluation of HDC-1 and HDC-3 as potential lead metabolites.

3.2. Network Pharmacology and Molecular Docking Analysis of HDC-1 and HDC-3 Against Inflammatory Bowel Disease

A network pharmacology approach integrating target prediction, protein–protein interaction analysis, functional enrichment, and molecular docking was used to investigate the potential mechanisms underlying the effects of HDC-1 and HDC-3 against inflammatory bowel disease (IBD). Potential

compound-related targets were retrieved from the PubChem and SwissTargetPrediction databases, whereas IBD-associated targets were collected from GeneCards and DisGeNET. The overlapping targets between each metabolite and IBD were identified using Venn diagram analysis and were subsequently selected for further investigation.

Protein–protein interaction networks were constructed using the STRING database to evaluate target connectivity and identify potentially important hub proteins. Gene Ontology and Kyoto Encyclopedia of Genes and Genomes pathway enrichment analyses were then performed to characterize the biological functions and signaling pathways associated with the overlapping targets.

The enrichment results indicated that the predicted targets of HDC-1 and HDC-3 were associated with inflammatory and immune-regulatory processes relevant to IBD. HDC-1 showed particularly strong enrichment in IBD-related pathways, whereas HDC-3 exhibited a broadly similar enrichment profile together with associations with several cancer-related pathways. These results suggest that the two metabolites may regulate multiple biological processes involved in intestinal inflammation.

Molecular docking was subsequently performed to evaluate the potential interactions of HDC-1 and HDC-3 with selected IBD-related target proteins. Both metabolites exhibited favorable predicted binding interactions with the investigated targets, involving amino acid residues such as Leu349, Phe400, Asn443, His439, and Thr470. The predicted interactions indicate that HDC-1 and HDC-3 may form stable complexes with selected target proteins through multiple non-covalent interactions.

Collectively, the network pharmacology and molecular docking results suggest that HDC-1 and HDC-3 may exert anti-IBD effects through multi-target and multi-pathway mechanisms involving inflammatory signaling, immune regulation, and intestinal barrier-associated processes. These computational findings provide a mechanistic basis for the experimentally observed anti-inflammatory effects of the deglycosylated HDC metabolites.

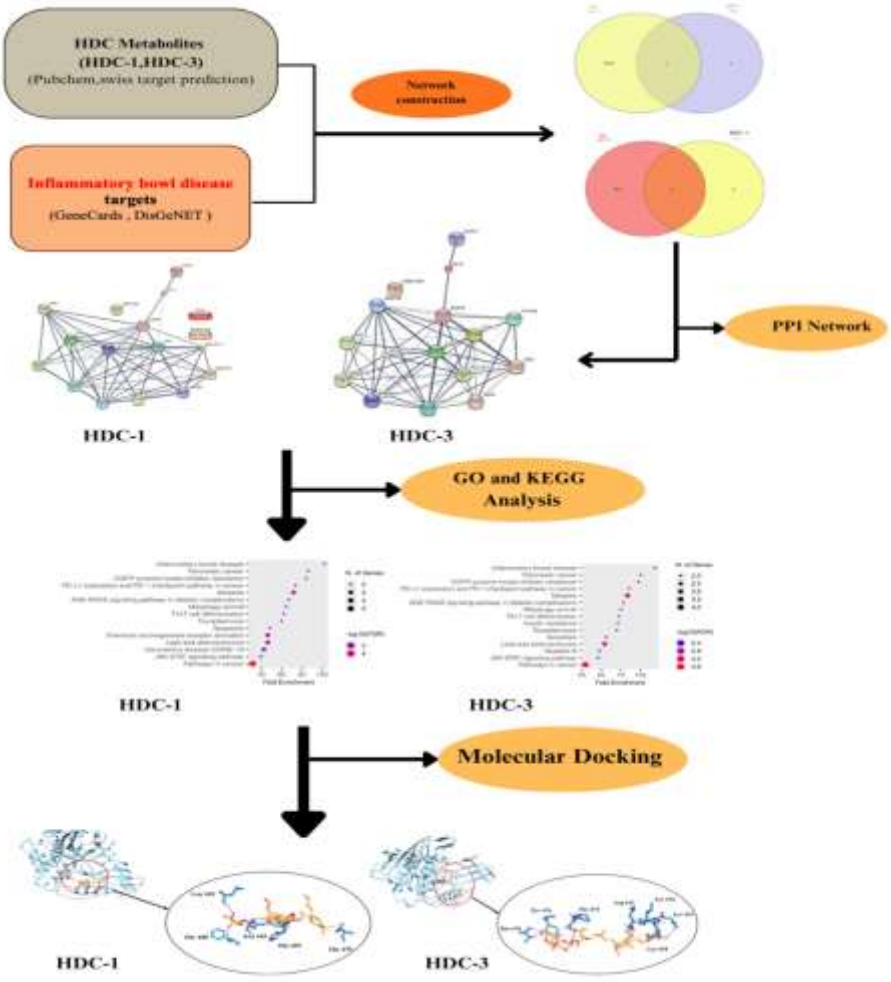

Figure 5. Network pharmacology and molecular docking analysis of HDC-1 and HDC-3 against inflammatory bowel disease.

3.3. In Vivo Evaluation of HDC-1 in DSS-Induced Colitis

Based on the in vitro screening results, HDC-1 and HDC-3 were identified as the most biologically active deglycosylated metabolites. HDC-1 was selected for in vivo evaluation because of its favorable combination of anti-inflammatory activity, preparative yield, and scalability. A dextran sulfate sodium (DSS)-induced murine colitis model was used to assess the therapeutic efficacy and dose-dependent effects of HDC-1. Mesalazine (5-aminosalicylic acid, 5-ASA), a commonly used first-line treatment for inflammatory bowel disease, was included as a positive control. Disease severity and therapeutic response were evaluated by monitoring body-weight changes, Disease Activity Index (DAI) scores, colon length, colonic concentrations of pro-inflammatory cytokines, and histopathological alterations (Figure 6).

Body-weight loss is a commonly used indicator of disease progression in DSS-induced colitis models [53,54]. In the DSS model group, body weight began to decrease continuously from day 5 and was significantly lower than that of the normal-control group from day 7 onward. Oral administration of HDC at 100 mg/kg and intraperitoneal administration of HDC-1 at 1.25, 2.5, or 5 mg/kg attenuated DSS-induced body-weight loss. The protective effect of HDC-1 was dose dependent, with the greatest improvement observed in the 5 mg/kg group. Body-weight recovery in this group became apparent by day 10. Under the tested experimental conditions, mesalazine at 200 mg/kg produced a less pronounced effect on body-weight loss than HDC-1.

The DAI, which incorporates body-weight loss, stool consistency, and rectal bleeding, was used to monitor clinical disease severity, with higher scores indicating more severe colitis [54]. DSS exposure significantly increased DAI scores compared with the normal-control group (Figure 6b). Treatment with oral HDC at 100 mg/kg or HDC-1 at 1.25, 2.5, and 5 mg/kg significantly reduced the DAI compared with the DSS model group. The greatest reduction was observed in mice treated with HDC-1 at 5 mg/kg. Under the dosing regimens used in this study, high-dose HDC-1 produced a greater improvement in DAI than oral HDC or mesalazine. These findings indicate that HDC-1 dose-dependently attenuated the clinical signs of DSS-induced colitis.

Colon shortening is a widely used macroscopic indicator of inflammation and tissue injury in experimental colitis [54]. DSS administration caused a significant reduction in colon length compared with the normal-control group (Figure 6c,d). Treatment with HDC, mesalazine, or HDC-1 partially reversed DSS-induced colon shortening. Among the treatment groups, HDC-1 at 5 mg/kg produced the most pronounced restoration of colon length. This effect was greater than that observed following oral administration of HDC or mesalazine under the tested conditions.

Pro-inflammatory cytokines are important indicators of intestinal inflammatory activity and therapeutic response [55]. DSS treatment significantly increased colonic IL-1β and IL-6 levels compared with the normal-control group (Figure 6e,f). HDC-1 treatment reduced both cytokines in a dose-dependent manner. Significant reductions in IL-1β were observed at HDC-1 doses of 2.5 and 5 mg/kg ($p < 0.01$), while IL-6 levels were also markedly decreased compared with the DSS model group. Oral HDC and mesalazine produced only modest reductions in IL-6 levels that did not reach statistical significance. These results indicate that HDC-1 effectively suppressed the colonic inflammatory response induced by DSS.

Histopathological examination provided further evidence of the protective effects of HDC-1 [54,56]. Hematoxylin and eosin staining showed intact mucosal epithelium, preserved crypt architecture, and an absence of marked inflammatory-cell infiltration or ulceration in the normal-control group (Figure 6g). In contrast, the DSS model group exhibited extensive mucosal damage, disruption and loss of crypts, crypt abscess formation, ulceration, and pronounced inflammatory-cell infiltration.

Treatment with HDC, mesalazine, or HDC-1 ameliorated these histopathological abnormalities to varying degrees. HDC-1 treatment preserved mucosal architecture, reduced inflammatory-cell infiltration, and promoted restoration of crypt structure in a dose-dependent manner. The most pronounced histological improvement was observed in the 2.5 and 5 mg/kg HDC-1 groups, in which inflammatory injury was markedly reduced and tissue morphology approached that of the normal-control group. Under the tested dosing regimens, the histopathological improvement produced by HDC-1 was greater than that observed with oral HDC or mesalazine.

Collectively, these findings demonstrate that HDC-1 attenuated DSS-induced experimental colitis in a dose-dependent manner. HDC-1 reduced body-weight loss and DAI scores, preserved colon length, suppressed colonic IL-1β and IL-6 production, and improved mucosal and crypt architecture. Although direct comparisons should be interpreted cautiously because HDC-1, HDC, and mesalazine were administered by different routes, the results support HDC-1 as a promising deglycosylated metabolite for further preclinical investigation.

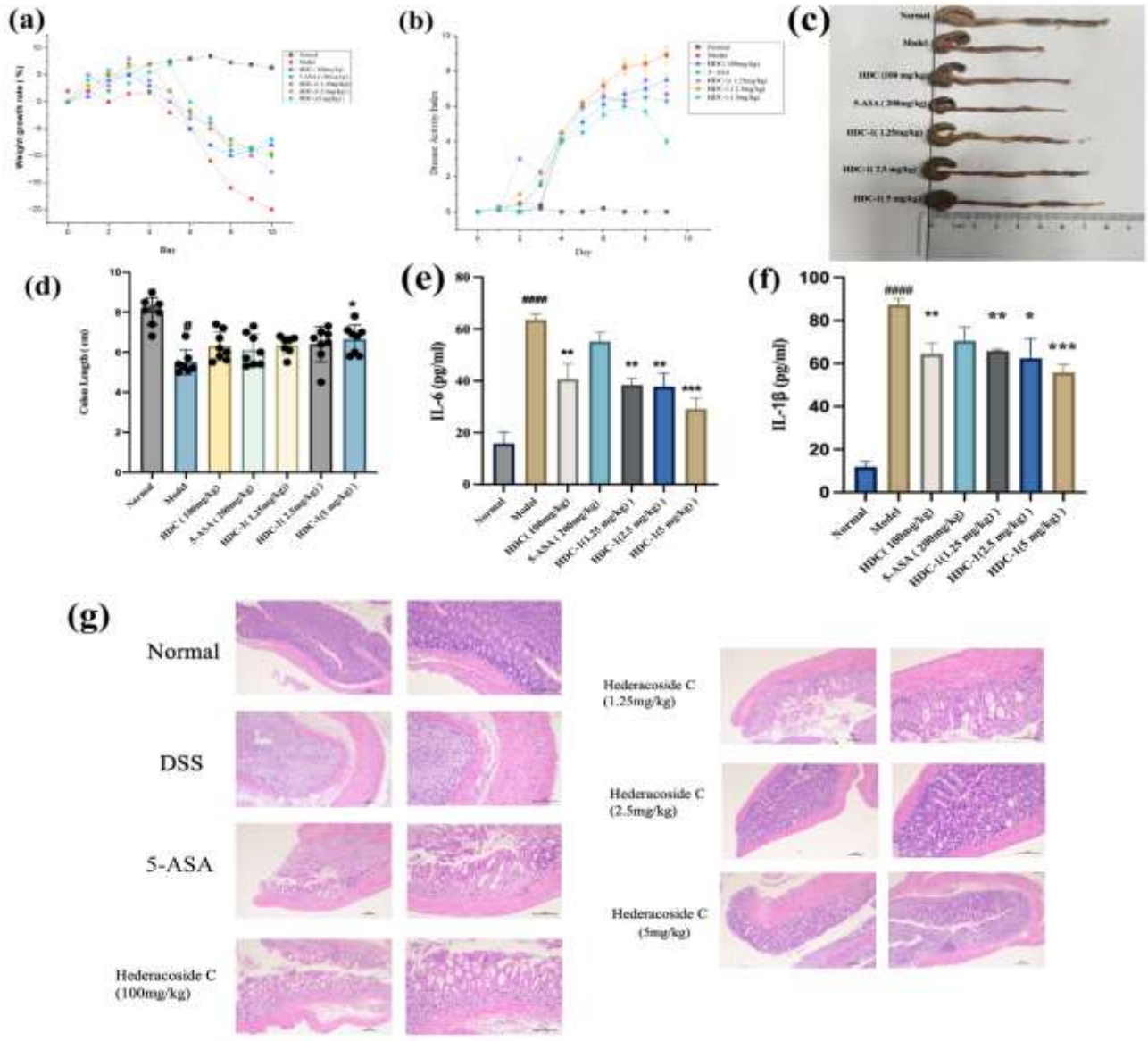

Figure 6. Therapeutic effects of HDC-1 in mice with DSS-induced colitis. (a) Changes in body weight during treatment; (b) Disease Activity Index (DAI) scores; (c) representative images of excised colons; (d) colon length; (e) colonic IL-1β levels; (f) colonic IL-6 levels; and (g) representative hematoxylin and eosin-stained sections of colonic tissue. Data are presented as the mean ± standard deviation (n = 8).

Если на рисунке используются символы статистической значимости, к подписи необходимо добавить их расшифровку, например:

#p < 0.05, ##p < 0.01 versus the normal-control group; *p < 0.05, **p < 0.01 versus the DSS model group.

Collectively, these findings indicate that HDC-1 attenuated DSS-induced colitis in a dose-dependent manner. Selective enzymatic removal of the terminal rhamnose residue from the C-28 glycosidic chain of Hederacoside C generated HDC-1, a partially deglycosylated metabolite with greater therapeutic activity than the parent compound under the experimental conditions used in this study. At the highest tested dose of HDC-1 (5 mg/kg), the nominal dose was 20-fold lower than that of oral HDC (100 mg/kg) and 40-fold lower than that of mesalazine (200 mg/kg). However, these comparisons should be interpreted cautiously because HDC-1 was administered intraperitoneally, whereas HDC and mesalazine were administered orally.

Inflammatory bowel disease, including ulcerative colitis and Crohn's disease, remains a major clinical challenge because of its chronic relapsing course and multifactorial pathogenesis involving genetic susceptibility, environmental factors, intestinal microbiota dysbiosis, epithelial barrier dysfunction, and abnormal immune activation

[57–60]. Although current therapies can induce and maintain remission in many patients, their effectiveness may be limited by primary non-response, secondary loss of response, adverse effects, and the need for long-term administration. Therefore, the development of new therapeutic candidates with improved pharmacological properties remains an important research priority.

Previous studies have shown that HDC can attenuate experimental intestinal inflammation through modulation of the S100A9/MAPK signaling axis, preservation of epithelial barrier integrity, and suppression of neutrophil recruitment and activation [40]. HDC has also been reported to inhibit NF-κB signaling, including the activation of p65 and IκBα, in experimental models of *Staphylococcus aureus*-induced inflammation [38]. These observations support the involvement of MAPK- and NF-κB-related pathways in the anti-inflammatory activity of HDC and its metabolites.

The present results demonstrate that HDC-1 exerted dose-dependent protective effects in DSS-induced colitis. Intraperitoneal administration of HDC-1 at 1.25–5 mg/kg reduced body-weight loss, decreased DAI scores, attenuated colon shortening, suppressed colonic IL-1β and IL-6 production, and improved histopathological injury. The highest dose of HDC-1 produced greater improvements in several disease-related outcomes than oral HDC or mesalazine under the tested dosing regimens. Nevertheless, direct conclusions regarding relative intrinsic potency require additional pharmacokinetic studies and comparisons using equivalent routes of administration.

Site-selective enzymatic deglycosylation substantially enhanced the biological activity of HDC, emphasizing the importance of glycosylation patterns in determining the pharmacological properties of triterpenoid saponins. Selective removal of the terminal rhamnose residue from the C-28 glycosidic chain may reduce molecular size and steric hindrance and may increase lipophilicity, membrane permeability, and target accessibility. However, these proposed mechanisms require confirmation through physicochemical, pharmacokinetic, and mechanistic investigations.

The enhanced activity of HDC-1 supports its further evaluation as a lead metabolite for the development of saponin-derived therapeutic candidates for inflammatory bowel disease. More broadly, the findings demonstrate that single-enzyme, site-selective deglycosylation can provide an efficient strategy for generating structurally defined metabolites with improved biological and drug-like properties from highly glycosylated natural products.

3.4. Preparative-Scale Enzymatic Production of HDC-1

Preparative-scale enzymatic production of HDC-1 was performed as a proof of concept for the scalable and environmentally sustainable manufacture of the metabolite. Under the optimized conditions, HDC (1.0 g; 20 mg/mL) was incubated with α-L-rhamnosidase RhaK at a final enzyme concentration of 38.4 U/mL at 50°C and pH 5.0 for 4 h.

Under these conditions, HDC-1 was the predominant reaction product. The process yielded approximately 0.4–0.5 g of purified HDC-1 from 1.0 g of starting HDC, corresponding to an isolated yield of approximately 40–50% (Figure 7). The product distribution and conversion efficiency were consistent with those observed in the smaller-scale experiments.

These results demonstrate that RhaK-mediated deglycosylation can selectively produce HDC-1 at the preparative scale under mild reaction conditions. The process avoids the strongly acidic conditions, nonspecific degradation, and extensive waste generation associated with conventional acid hydrolysis. Although further optimization of enzyme consumption, substrate concentration, reaction time, purification efficiency, and batch reproducibility is required, the present findings support the feasibility of developing an environmentally sustainable process for HDC-1 production and subsequent preclinical investigation.

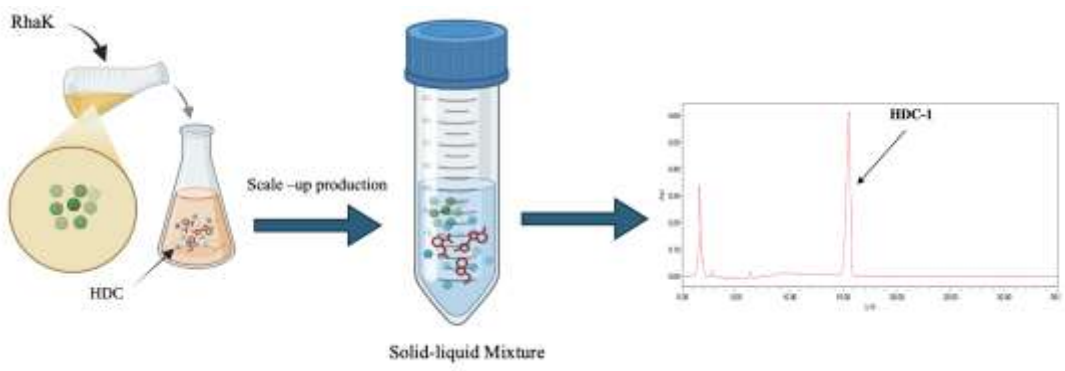

Figure 7. Preparative-scale enzymatic production of HDC-1 from Hederacoside C using α-L-rhamnosidase RhaK under optimized reaction conditions.

3.5. Limitations and Future Directions

This study has several limitations. First, the in vivo efficacy of HDC-1 was evaluated only after intraperitoneal administration in an acute dextran sulfate sodium-induced murine colitis model. This model does not fully reproduce the chronic, relapsing, and heterogeneous nature of human inflammatory bowel disease. Moreover, HDC-1 was administered by a different route from the parent compound HDC and mesalazine, which limits direct comparisons of their relative potency and therapeutic efficacy.

Second, comprehensive pharmacokinetic studies were not performed. Consequently, the absorption, distribution, metabolism, elimination, systemic exposure, and oral bioavailability of HDC-1 remain unknown. Long-term toxicity, immunogenicity, and safety following repeated administration were also not evaluated. In addition, only HDC-1 was examined in vivo, although HDC-3 showed substantial anti-inflammatory activity in the in vitro experiments.

Third, the molecular mechanisms underlying the enhanced biological activity of HDC-1 have not been fully elucidated. Although the network pharmacology and molecular docking analyses identified several potential targets and pathways, these computational predictions require experimental validation. Furthermore, the proposed effects of deglycosylation on lipophilicity, membrane permeability, and target accessibility were not directly measured.

Future studies should focus on developing suitable oral formulations of HDC-1 and evaluating its efficacy in chronic and relapsing models of colitis. Detailed pharmacokinetic, oral bioavailability, absorption, distribution, metabolism, excretion, and safety studies are also required. Comparative studies using equivalent administration routes should be performed to allow a more reliable assessment of HDC-1 relative to HDC and established IBD therapies. Mechanistic investigations integrating transcriptomic analysis, intestinal microbiota profiling, pathway validation, and structure–activity relationship studies may further clarify the biological effects of selective deglycosylation. These studies will be essential for determining the preclinical development potential of HDC-1 and related saponin-derived metabolites.

4. Conclusion

This study established a single-enzyme, site-selective deglycosylation approach using α-L-rhamnosidase RhaK to generate three principal metabolites of Hederacoside C, designated HDC-1, HDC-2, and HDC-3. Compared with conventional acid hydrolysis, the enzymatic process provided greater selectivity, produced a cleaner metabolite profile, and operated under milder reaction conditions. HDC-1 and HDC-3 exhibited the most pronounced biological activities in vitro, including protection against erastin-induced ferroptotic injury and inhibition of LPS-induced IL-1β and IL-6 production.

HDC-1 was selected for in vivo evaluation because of its favorable combination of biological activity, preparative yield, and scalability. In the DSS-induced murine colitis model, intraperitoneal administration of HDC-1 at 1.25–5 mg/kg dose-dependently reduced body-weight loss and Disease Activity Index scores, attenuated colon shortening, decreased colonic IL-1β and IL-6 levels, and improved histopathological injury. Under the tested dosing regimens, HDC-1 produced greater improvements in several disease-related outcomes than oral HDC at 100 mg/kg or mesalazine at 200 mg/kg. However, these comparisons should be interpreted cautiously because the compounds were administered by different routes.

Preparative-scale conversion of 1.0 g of HDC yielded approximately 0.4–0.5 g of purified HDC-1, supporting the feasibility of further process development. Overall, the findings demonstrate that selective removal of terminal rhamnose residues can enhance the biological activity of HDC and identify HDC-1 as a promising lead metabolite for further preclinical investigation. The study also supports enzymatic deglycosylation as an environmentally sustainable strategy for generating structurally defined and biologically active derivatives of highly glycosylated triterpenoid saponins. Additional pharmacokinetic, oral formulation, chronic efficacy, safety, and mechanistic studies are required before the therapeutic potential of HDC-1 can be fully established.

Declarations

Author Contributions: Sabiqun Nahar Bithy: Investigation , Data curation , Methodology, Writing. Ra Ade Hossain: Language polishing, editing; Jianqin Zhou: Funding acquisition, Methodology; Yanli Liu: Conceptualization, Writing-review & editing. Qiongming Xu: Funding acquisition, Conceptualization, Writing-review & editing. All the authors have read and approved the final manuscript.

Conflicts of interest

There are no conflicts to declare.

Acknowledgements

This work was supported by the National Natural Science Foundation of China (32371550, 82574288, 82341087), and Priority Academic Program Development of Jiangsu Higher Education Institutions (PAPD).

References

[1] Upadhyay, S., et al., Inflammatory bowel diseases (IBDs), in Targeting Angiogenesis, Inflammation, and Oxidative Stress in Chronic Diseases. 2024, Elsevier. p. 93–108.

[2] Deshmukh, R., S. Kumari, and R.K. Harwansh, Inflammatory bowel disease: A snapshot of current knowledge. Research Journal of Pharmacy and Technology, 2020. 13(2): p. 956–962.

[3] Deshmukh, C.D., A review on inflammatory bowel disease. Asian J Pharm Clin Res, 2023. 16(6): p. 11–14.

[4] Vuyyuru, S.K., et al., Immune-mediated inflammatory diseases of the gastrointestinal tract: Beyond Crohn's disease and ulcerative colitis. JGH Open, 2022. 6(2): p. 100–111.

[5] Al-Dabbagh, I.S., Comprehensive Insight into Crohn's Disease: Diagnosis, Clinical Presentation, Complications and Treatment". Journal of the College of Basic Education, 2025. 1(المؤتمر وقائع الأسا التربية لكلية العلمي): p. 65–82.

[6] Diez-Martin, E., et al., Inflammatory bowel disease: a comprehensive analysis of molecular bases, predictive biomarkers, diagnostic methods, and therapeutic options. International Journal of Molecular Sciences, 2024. 25(13): p. 7062.

[7] Silaghi, A., et al., Inflammatory bowel disease: pathogenesis, diagnosis and current therapeutic approach. Journal of Mind and Medical Sciences, 2022. 9(1): p. 5.

[8] Libertucci, J., et al., Inflammation-related differences in mucosa-associated microbiota and intestinal barrier function in colonic Crohn's disease. American Journal of Physiology-Gastrointestinal and Liver Physiology, 2018. 315(3): p. G420–G431.

[9] Yangyang, R.Y. and J.R. Rodriguez. Clinical presentation of Crohn's, ulcerative colitis, and indeterminate colitis: Symptoms, extraintestinal manifestations, and disease phenotypes. in Seminars in pediatric surgery. 2017. Elsevier.

[10] Gros, B. and G.G. Kaplan, Ulcerative colitis in adults: a review. Jama, 2023. 330(10): p. 951–965.

[11] De Deo, D., et al., Management of proctitis in ulcerative colitis and the place of biological therapies. Expert Opinion on Biological Therapy, 2024. 24(6): p. 443–453.

[12] Sange, A.H., et al., Extra-intestinal manifestations of inflammatory bowel disease. Cureus, 2021. 13(8).

[13] Faggiani, I., et al., Extraintestinal manifestations in inflammatory bowel disease: from pathophysiology to treatment. Biomedicines, 2024. 12(8): p. 1839.

[14] Glyn, T. and A.L. Lightner, Inflammatory Bowel Disease and Colorectal Cancer. Digestive disease interventions, 2023. 7(01): p. 051–057.

[15] Armuzzi, A. and G. Liguori, Quality of life in patients with moderate to severe ulcerative colitis and the impact of treatment: a narrative review. Digestive and Liver Disease, 2021. 53(7): p. 803–808.

[16] Santana, P.T., et al., Dysbiosis in inflammatory bowel disease: pathogenic role and potential therapeutic targets. International journal of molecular sciences, 2022. 23(7): p. 3464.

[17] Neurath, M.F., Strategies for targeting cytokines in inflammatory bowel disease. Nature Reviews Immunology, 2024. 24(8): p. 559–576.

[18] Vebr, M., et al., A narrative review of cytokine networks: pathophysiological and therapeutic implications for inflammatory bowel disease pathogenesis. Biomedicines, 2023. 11(12): p. 3229.

[19] Ju, L., et al., Fecal microbiota and metabolites in the pathogenesis and precision medicine for inflammatory bowel disease. Precision Clinical Medicine, 2024. 7(3): p. pbae023.

[20] Guan, Q., A comprehensive review and update on the pathogenesis of inflammatory bowel disease. Journal of immunology research, 2019. 2019(1): p. 7247238.

[21] Liu, J., B. Di, and L.-l. Xu, Recent advances in the treatment of IBD: targets, mechanisms and related therapies. Cytokine & growth factor reviews, 2023. 71: p. 1–12.

[22] Imbrizi, M., F. Magro, and C.S.R. Coy, Pharmacological therapy in inflammatory bowel diseases: a narrative review of the past 90 years. Pharmaceuticals, 2023. 16(9): p. 1272.

[23] Imbrizi, M., et al., Positioning and sequencing of advanced therapies in inflammatory bowel disease: A guide for clinical practice. World Journal of Gastroenterology, 2025. 31(29): p. 107745.

[24] Wang, L.-F., et al., Predictors and optimal management of tumor necrosis factor antagonist nonresponse in inflammatory bowel disease: A literature review. World Journal of Gastroenterology, 2023. 29(29): p. 4481.

[25] Bonovas, S., et al., Biologic therapies and risk of infection and malignancy in patients with inflammatory bowel disease: a systematic review and network meta-analysis. Clinical Gastroenterology and Hepatology, 2016. 14(10): p. 1385–1397. e10.

[26] Quezada, S.M., L.P. McLean, and R.K. Cross, Adverse events in IBD therapy: the 2018 update. Expert review of gastroenterology & hepatology, 2018. 12(12): p. 1183–1191.

[27] Jamtsho, T., A. Loukas, and P. Wangchuk, Pharmaceutical Potential of Remedial Plants and Helminths for Treating Inflammatory Bowel Disease. Pharmaceuticals, 2024. 17(7): p. 819.

[28] Babalola, O.O., et al., Integrating phytochemicals and in silico methods for modern

drug discovery: a comprehensive review. Discover Chemistry, 2025. 2(1): p. 297.
[29] Karalija, E., A. Macanović, and S. Ibragić, Revisiting traditional medicinal plants: integrating multiomics, in vitro culture, and elicitation to unlock bioactive potential. Plants, 2025. 14(13): p. 2029.
[30] Cheng, W.-W., et al., Natural products on inflammatory bowel disease: Role of gut microbes. The American Journal of Chinese Medicine, 2024. 52(05): p. 1275–1301.
[31] Xie, L., et al., The pharmacology and mechanisms of platycodin D, an active triterpenoid saponin from Platycodon grandiflorus. Frontiers in Pharmacology, 2023. 14: p. 1148853.
[32] Wang, Y.H., Naturally occurring polyhydroxylated spirostanol saponins, a review of the classification, sources, biosynthesis, biological activities, and toxicity. Chemistry & Biodiversity, 2025. 22(1): p. e202401720.
[33] Chauhan, S., et al., Bioactive natural leads and traditional herbal plants in the management of inflammatory bowel diseases: a brief review. Letters in Drug Design & Discovery, 2024. 21(12): p. 2288–2301.
[34] Guo, C., et al., Plant defense mechanisms against ozone stress: Insights from secondary metabolism. Environmental and Experimental Botany, 2024. 217: p. 105553.
[35] Akhtar, M., et al., Hederacoside-C inhibition of Staphylococcus aureus-induced mastitis via TLR2 & TLR4 and their downstream signaling NF-κB and MAPKs pathways in vivo and in vitro. Inflammation, 2020. 43(2): p. 579–594.
[36] Xu, H.-c., et al., Hederacoside-C protects against AGEs-induced ECM degradation in mice chondrocytes. International Immunopharmacology, 2020. 84: p. 106579.
[37] Shokry, A.A., et al., In-depth molecular assessment of Hedera helix's L. α–Hederin & Hederacoside C as a gastroprotective & a possible safe Omeprazole phyto-alternative in ethanol-induced gastric ulcer mice model. International Immunopharmacology, 2025. 156: p. 114541.
[38] Akhtar, M., et al., Anti-inflammatory effects of Hederacoside-C on Staphylococcus aureus induced inflammation via TLRs and their downstream signal pathway in vivo and in vitro. Microbial Pathogenesis, 2019. 137: p. 103767.
[39] Muhammad, A., et al., Hederacoside-C inhibition of staphylococcus aureus-induced mastitis via TLR2 & TLR4 and their downstream Signaling NF-κB and MAPKs pathways in vivo and in vitro. Inflammation, 2020. 43(2): p. 579–594.
[40] Zha, Z.-x., et al., Hederacoside C ameliorates colitis via restoring impaired intestinal barrier through moderating S100A9/MAPK and neutrophil recruitment inactivation. Acta Pharmacologica Sinica, 2023. 44(1): p. 105–119.
[41] Kim, J.M., et al., Pharmacokinetics of hederacoside C, an active ingredient in AG NPP709, in rats. Xenobiotica, 2013. 43(11): p. 985–992.
[42] Yu Miao, Y.M., et al., Pharmacokinetic parameters of three active ingredients hederacoside C, hederacoside D, and α-hederin in Hedera helix in rats. 2016.
[43] Ko, H., et al., Separation and Cytotoxicity of Enzymatic Transformed Prosaikogenins from Bupleurum falcatum. Planta Medica, 2025. 91(10/11): p. 590–598.
[44] Hu, Y., et al., Triazole derivatives as potential antifungal agents: A structure-activity relationship (SAR) studies. Process Biochemistry, 2023. 135: p. 102–118.
[45] Ramalingam, V., et al., Chemical fabrication of graphene oxide nanosheets attenuates biofilm formation of human clinical pathogens. Bioorganic chemistry, 2019. 83: p. 326–335.
[46] Bodakowska-Boczniewicz, J. and Z. Garncarek, Characterization of α-L-Rhamnosidase and β-D-Glucosidase Subunits of Naringinase Immobilized on a Magnetic Polysaccharide Carrier. International Journal of Molecular Sciences, 2025. 26(19): p. 9813.
[47] Cui, C.-H., et al., A Novel Ginsenoside-Transforming α-L-Rhamnosidase from Bifidobacterium: Screening, Characterization and Application. Biomolecules, 2024. 14(12): p. 1611.
[48] Liu, C., et al., Multifaceted interplays between the essential players and lipid peroxidation in ferroptosis. Journal of Genetics and Genomics, 2025.
[49] Liu, R., Q. Luo, and G. Song, Ferroptosis: A key regulator and potential target for tissue injury. Histol. Histopathol, 2025. 40(6): p. 813–823.
[50] Cheng, Q., et al., Erastin synergizes with cisplatin via ferroptosis to inhibit ovarian cancer growth in vitro and in vivo. Journal of obstetrics and gynaecology research, 2021. 47(7): p. 2481–2491.
[51] Li, Y., et al., Erastin induces ferroptosis via ferroportin-mediated iron accumulation in endometriosis. Human Reproduction, 2021. 36(4): p. 951–964.
[52] Chen, X.L., et al., Alkaloid Components From Orychophragmus violaceus and Their Ferroptosis Inhibition Activity. Chemistry & Biodiversity, 2026. 23(1): p. e03337.
[53] Silva, N.-V., et al., A dietary cholesterol-based intestinal inflammation assay for improving drug-discovery on inflammatory bowel diseases. Frontiers in Cell and Developmental Biology, 2021. 9: p. 674749.
[54] Feng, W., et al., Anemoside B4 ameliorates dextran sulfate sodium (DSS)-induced colitis through

inhibiting NLRP3 inflammasome and modulating gut microbiota. European Journal of Pharmacology, 2024. 963: p. 176164.
[55] Wu, H., et al., Anemoside B4 alleviates ulcerative colitis by attenuating intestinal oxidative stress and NLRP3 inflammasome via activating aryl hydrocarbon receptor through remodeling the gut microbiome and metabolites. Redox Biology, 2025. 85: p. 103746.
[56] Langner, C., et al., The histopathological approach to inflammatory bowel disease: a practice guide. Virchows Archiv, 2014. 464(5): p. 511–527.
[57] Bai, J., et al., Gene-Environment interactions in inflammatory bowel disease: A systematic review of human epidemiologic studies. Journal of Crohn's and Colitis, 2025. 19(6): p. jjaf061.
[58] Calvez, V., et al., Novel insights into the pathogenesis of inflammatory bowel diseases. Biomedicines, 2025. 13(2): p. 305.
[59] Ramos, G.P. and K.A. Papadakis. Mechanisms of disease: inflammatory bowel diseases. in Mayo Clinic Proceedings. 2019. Elsevier.
[60] Basso, P., et al., Association among genetic predisposition, gut microbiota, and host immune response in the etiopathogenesis of inflammatory bowel disease. Brazilian Journal of Medical and Biological Research, 2014. 47(9): p. 727–737.

参考文:

[1] Upadhyay, S. 等，炎症性肠病（IBD），载于《慢性疾病中的血管生成、炎症与氧化应激靶向治疗》。Elsevier，2024年，第93–108页。
[2] Deshmukh, R.、S. Kumari 和 R.K. Harwansh，炎症性肠病：当前知识概览。《药学与技术研究杂志》，2020年，第13卷第2期，第956–962页。
[3] Deshmukh, C.D.，炎症性肠病综述。《亚洲药学与临床研究杂志》，2023年，第16卷第6期，第11–14页。
[4] Vuyyuru, S.K. 等，胃肠道免疫介导性炎症性疾病：超越克罗恩病和溃疡性结肠炎。《JGH Open》，2022年，第6卷第2期，第100–111页。
[5] Al-Dabbagh, I.S.，克罗恩病的全面认识：诊断、临床表现、并发症与治疗。《基础教育学院学报》，2025年，第1期（وقائع المؤتمر العلمي لكلية التربية الأسا），第65–82页。
[6] Diez-Martin, E. 等，炎症性肠病：分子基础、预测性生物标志物、诊断方法和治疗选择的综合分析。《国际分子科学杂志》，2024年，第25卷第13期，文章编号7062。
[7] Silaghi, A. 等，炎症性肠病： 发病机制、诊断及当前治疗方法。《心智与医学科学杂志》，2022年，第9卷第1期，第5页。
[8] Libertucci, J. 等，结肠型克罗恩病中黏膜相关微生物群和肠道屏障功能的炎症相关差异。《美国生理学杂志：胃肠与肝脏生理学》，2018年，第315卷第3期，第G420–G431页。
[9] Yangyang, R.Y. 和 J.R. Rodriguez，克罗恩病、溃疡性结肠炎及未定型结肠炎的临床表现：症状、肠外表现和疾病表型。载于《小儿外科专题研讨》，Elsevier，2017年。
[10] Gros, B. 和 G.G. Kaplan，成人溃疡性结肠炎：综述。《美国医学会杂志》，2023年，第330卷第10期，第951–965页。
[11] De Deo, D. 等，溃疡性结肠炎直肠炎的管理及生物治疗的地位。《生物治疗专家评论》，2024年，第24卷第6期，第443–453页。
[12] Sange, A.H. 等，炎症性肠病的肠外表现。《Cureus》，2021年，第13卷第8期。
[13] Faggiani, I. 等，炎症性肠病的肠外表现：从病理生理学到治疗。《生物医学》，2024年，第12卷第8期，文章编号1839。
[14] Glyn, T. 和 A.L. Lightner，炎症性肠病与结直肠癌。《消化系统疾病干预》，2023年，第7卷第1期，第51–57页。
[15] Armuzzi, A. 和 G. Liguori，中重度溃疡性结肠炎患者的生活质量及治疗影响：叙述性综述。《消化与肝脏疾病》，2021年，第53卷第7期，第803–808页。
[16] Santana, P.T. 等，炎症性肠病中的菌群失调：致病作用及潜在治疗靶点。《国际分子科学杂志》，2022年，第23卷第7期，文章编号3464。
[17] Neurath, M.F.，炎症性肠病中靶向细胞因子的策略。《自然评论：免疫学》，2024年，第24卷第8期，第559–576页。
[18] Vebr, M. 等，细胞因子网络的叙述性综述：炎症性肠病发病机制中的病理生理学及治疗意义。《生物医学》，2023年，第11卷第12期，文章编号3229。
[19] Ju, L. 等，炎症性肠病发病机制及精准医学中的粪便微生物群与代谢物。《精准临床医学》，2024年，第7卷第3期，文章编号pbae023。
[20] Guan, Q.，炎症性肠病发病机制的全面综述与最新进展。《免疫学研究杂志》，2019年，第2019卷第1期，文章编号7247238。

[21] Liu, J.、B. Di 和 L.-l. Xu，炎症性肠病治疗的最新进展：靶点、机制及相关疗法。《细胞因子与生长因子评论》，2023年，第71卷，第1–12页。

[22] Imbrizi, M.、F. Magro 和 C.S.R. Coy，炎症性肠病的药物治疗：过去90年的叙述性综述。《药物学》，2023年，第16卷第9期，文章编号1272。

[23] Imbrizi, M. 等，炎症性肠病先进疗法的定位与序贯应用：临床实践指南。《世界胃肠病学杂志》，2025年，第31卷第29期，文章编号107745。

[24] Wang, L.-F. 等，炎症性肠病中肿瘤坏死因子拮抗 剂无应答的预测因素及最佳管理：文献综述。《世界胃肠病学杂志》，2023年，第29卷第29期，第4481页。

[25] Bonovas, S. 等，炎症性肠病患者接受生物治疗后的 感染和恶性肿瘤风险：系统综述与网络荟萃分析。《临床胃肠病学与肝病学》，2016年，第14卷第10期，第1385–1397页，e10。

[26] Quezada, S.M.、L.P. McLean 和 R.K. Cross，炎症性肠病治疗中的不良事件：2018年更新。《胃肠病学与肝病学专家评论》，2018年，第12卷第12期，第1183–1191页。

[27] Jamtsho, T.、A. Loukas 和 P. Wangchuk，药用植物与蠕虫治疗炎症性肠病的药用潜力。《药物学》，2024年，第17卷第7期，文章编号819。

[28] Babalola, O.O. 等，将植物化学成分与计算机模拟方法整合用于现代药物发现：综合综述。《发现化学》，2025年，第2卷第1期，文章编号297。

[29] Karalija, E.、A. Macanović 和 S. Ibragić，重新审视传统药用植物：整合多组学、体外培养与诱导技术以开发生物活性潜力。《植物》，2025年，第14卷第13期，文章编号2029。

[30] Cheng, W.-W. 等，天然产物对炎症性肠病的作用：肠道微生物的角色。《美国中医药杂志》，2024年，第52卷第5期，第1275–1301页。

[31] Xie, L. 等，桔梗活性三萜皂苷桔梗皂苷D的药理作用及机制。《药理学前沿》，2023年，第14卷，文章编号1148853。

[32] Wang, Y.H.，天然多羟基螺甾烷型皂苷：分类、来源、生物合成、生物活性及毒性综述。《化学与生物多样性》，2025年，第22卷第1期，文章编号e202401720。

[33] Chauhan, S. 等，生物活性天然先导化合物和传统草药在炎症性肠病管理中的应用：简要综述。《药物设计与发现快报》，2024年，第21卷第12期，第2288–2301页。

[34] Guo, C. 等，植物抵御臭氧胁迫的防御机制：来自次生代谢的认识。《环境与实验植物学》，2024年，第217卷，文章编号105553。

[35] Akhtar, M. 等，常春藤皂苷C通过TLR2、TLR4及其下游NF-κB和MAPK信号通路抑制金黄色葡萄球菌诱导的乳腺炎：体内与体外研究。《炎症》，2020年，第43卷第2期，第579–594页。

[36] Xu, H.-c. 等，常春藤皂苷C保护小鼠软骨细胞免受晚期糖基化终末产物诱导的细胞外基质降解。《国际免疫药理学》，2020年，第84卷，文章编号106579。

[37] Shokry, A.A. 等，常春藤中α-常春藤皂苷和常春藤皂苷C作为胃黏膜保护剂及安全奥美拉唑植物替代物的深入分子评价：乙醇诱导小鼠胃溃疡模型研究。《国际免疫药理学》，2025年，第156卷，文章编号114541。

[38] Akhtar, M. 等，常春藤皂苷C通过TLR及其下游信号通路抑制金黄色葡萄球菌诱导炎症的抗炎作用：体内与体外研究。《微生物致病机制》，2019年，第137卷，文章编号103767。

[39] Muhammad, A. 等，常春藤皂苷C通过TLR2、TLR4及其下游NF-κB和MAPK信号通路抑制金黄色葡萄球菌诱导的乳腺炎：体内与体外研究。《炎症》，2020年，第43卷第2期，第579–594页。

[40] Zha, Z.-x. 等，常春藤皂苷C通过调控S100A9/MAPK通路并抑制中性粒细胞募集，恢复受损的肠道屏障，从而改善结肠炎。《中国药理学报》，2023年，第44卷第1期，第105–119页。

[41] Kim, J.M. 等，AG NPP709活性成分常春藤皂苷C在大鼠体内的药代动力学。《异生物质》，2013年，第43卷第11期，第985–992页。

[42] Yu Miao, Y.M. 等，常春藤中三种活性成分常春藤皂苷C、常春藤皂苷D和α-常春藤皂苷在大鼠体内的药代动力学参数。2016年。

[43] Ko, H. 等，柴胡中经酶转化的原柴胡皂苷元的分离及细胞毒性。《药用植物》，2025年，第91卷第10/11期，第590–598页。

[44] Hu, Y. 等，作为潜在抗真菌药物的三唑衍生物：构效关系研究。《过程生物化学》，2023年，第135卷，第102–118页。

[45] Ramalingam, V. 等，化学制备的氧化石墨烯纳米片可抑制人类临床病原体的生物膜形成

。《生物有机化学》，2019年，第83卷，第326–335页。
[46] Bodakowska-Boczniewicz, J. 和 Z. Garncarek，固定于磁性多糖载体上的柚皮苷酶α-L-鼠李糖苷酶和β-D-葡萄糖苷酶亚基的表征。《国际分子科学杂志》，2025年，第26卷第19期，文章编号9813。
[47] Cui, C.-H. 等，来源于双歧杆菌的新型人参皂苷转化α-L-鼠李糖苷酶：筛选、表征与应用。《生物分子》，2024年，第14卷第12期，文章编号1611。
[48] Liu, C. 等，铁死亡中关键调控因子与脂质过氧化之间的多层次相互作用。《遗传学与基因组学杂志》，2025年。
[49] Liu, R.、Q. Luo 和 G. Song，铁死亡：组织损伤的关键调控机制及潜在治疗靶点。《组织学与组织病理学》，2025年，第40卷第6期，第813–823页。
[50] Cheng, Q. 等，Erastin通过铁死亡与顺铂协同作用，在体内外抑制卵巢癌生长。《妇产科学研究杂志》，2021年，第47卷第7期，第2481–2491页。
[51] Li, Y. 等，Erastin通过铁转运蛋白介导的铁积累诱导子宫内膜异位症细胞发生铁死亡。《人类生殖》，2021年，第36卷第4期，第951–964页。
[52] Chen, X.L. 等，诸葛菜中的生物碱成分及其铁死亡抑制活性。《化学与生物多样性》，2026年，第23卷第1期，文章编号e03337。
[53] Silva, N.-V. 等，基于膳食胆固醇的肠道炎症检测方法，用于改进炎症性肠病药物发现。《细胞与发育生物学前沿》，2021年，第9卷，文章编号674749。
[54] Feng, W. 等，白头翁皂苷B4通过抑制NLRP3炎性小体并调节肠道微生物群改善葡聚糖硫酸钠诱导的结肠炎。《欧洲药理学杂志》，2024年，第963卷，文章编号176164。
[55] Wu, H. 等，白头翁皂苷B4通过重塑肠道微生物群及其代谢物激活芳香烃受体，减轻肠道氧化应激并抑制NLRP3炎性小体，从而缓解溃疡性结肠炎。《氧化还原生物学》，2025年，第85卷，文章编号103746。
[56] Langner, C. 等，炎症性肠病的组织病理学诊断方法：实践指南。《Virchows档案》，2014年，第464卷第5期，第511–527页。
[57] Bai, J. 等，炎症性肠病中的基因—环境相互作用：人类流行病学研究的系统综述。《克罗恩病与结肠炎杂志》，2025年，第19卷第6期，文章编号jjaf061。
[58] Calvez, V. 等，炎症性肠病发病机制的新见解。《生物医学》，2025年，第13卷第2期，文章编号305。
[59] Ramos, G.P. 和 K.A. Papadakis，疾病机制：炎症性肠病。载于《梅奥诊所学报》，Elsevier，2019年。
[60] Basso, P. 等，遗传易感性、肠道微生物群与宿主免疫反应在炎症性肠病病因及发病机制中的关联。《巴西医学与生物学研究杂志》，2014年，第47卷第9期，第727–737页。

Manuscript Information
Word count: 12,253 words (excluding references).
Peer-Review Record

Fast-track status: Not fast-tracked.
First-round reviews received: 3 reports.
Revision cycles completed: 3 rounds.
Final version submitted: July 6, 2026